A Study of Diamond-Like Carbon Thin Films Prepared by Microwave Plasma Chemical Vapour Deposition

2007 Plasma Sci. Technol. 9 444

(http://iopscience.iop.org/1009-0630/9/4/13)

A Study of Diamond-Like Carbon Thin Films Prepared by Microwave Plasma Chemical Vapour Deposition*

LAI Xiuqiong (赖秀琼), CHEN Junfang (陈俊芳), FU Silie(符斯列), LI Wei (李炜), ZHANG Maoping(张茂平), SHI Lei(史磊), YANG Chunlin(杨春林)

School of Physics and Telecommunication Engineering, South China Normal University Guangdong 510631, China

Abstract In order to deposit good films, we need to study the uniformity of plasma density and the plasma density under different gas pressures and powers. The plasma density was diagnosed by a Langmuir probe. The optical emission spectroscopy (OES) of CH_4 and H_2 discharge was obtained with raster spectroscopy, with characteristic peaks of H and CH achieved. Diamond-like carbon films were achieved based on the study of plasma density and OES and characterized by atomic force microscope (AFM), X-ray diffraction instrument (XRD), Raman spectroscope and profiler.

Keywords: plasma density, Langmuir probe, OES, diamond-like carbon thin films

PACS: *52.70.-m, 52.70.Kz, 52.50.Qt*

1 Introduction

Diamond-like carbon thin films have outstanding properties such as extreme hardness, high electric resistivity, optical transparency in the infrared region, and high chemical inertness [1~3].

Different techniques are used to prepare diamond-like carbon (DLC) films. In this study, we used microwave plasma chemical vapour deposition (MPCVD). Microwave discharge is non-electrode. It can obtain pure and high density plasma. For the same gas discharge, microwave can excite and ionize more gas molecules. Furthermore, microwave discharge can be operated stably in a wide range of gas pressure, and therefore has extensive applications [4~6].

As plasma has a certain spatial distribution, in order to deposit even, pure and high quality thin films, we need to investigate the uniformity of the plasma distribution in the reaction chamber.

For the diagnosis of the plasma, a Langmuir probe is often used to measure the characteristic parameters of plasma. In this work, we used a Langmuir probe to diagnose the spatial plasma density distribution in the reaction chamber of the quartz tube microwave plasma apparatus and analysed its distribution characteristics.

With OES of H_2 and CH_4 discharge, we also examined the state of the chemical species present in the plasma.

2 Experimental apparatus

A schematic diagram of the quartz tube microwave plasma apparatus is shown in Fig. 1.

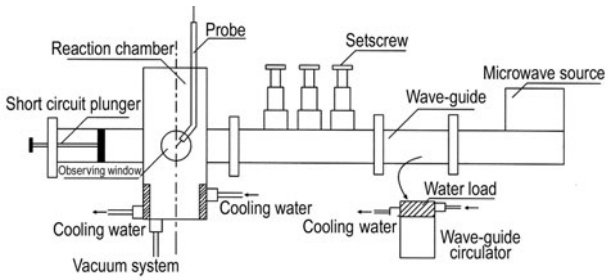

Fig.1 Schematic diagram of the quartz tube microwave plasma apparatus

The apparatus employs microwave at a frequency of 2.45 GHz to excite a gas discharge and generate the plasma. The waveguide is of the BJ22 type, and its working pattern is TE_{10}.

We used a Langmuir probe to diagnose the plasma, as shown in Fig. 2. A tungsten probe with a diameter of 0.8 mm was covered with a stainless steel tube and insulated by ceramics. To measure the plasma density in different radial positions, we first fixed an axial position and radial position at $R = -16$ mm, then started from this position and revolved the probe head by a calculated angle. After that, we changed the axial position and repeated the above operation to obtain the spatial plasma density.

The electron temperature T_e is given by the formula:

$$kT_e = \left| \mathrm{d}(eU_p)/\mathrm{d}\ln(I_p) \right|,$$

where U_p and I_p are the probe voltage and the collected electric probe current respectively.

The plasma density N_i is then given by

*supported in part by the National Natural Science Foundation of China (10575039), the Chinese Specialized Research Fund for the Doctoral Programme of Higher Education (2004057408), the Key Project of Science Research Fund of Guangdong (China) (05100534), and the Science Project Foundation of Guangzhou City (China) (2005Z3-D2031).

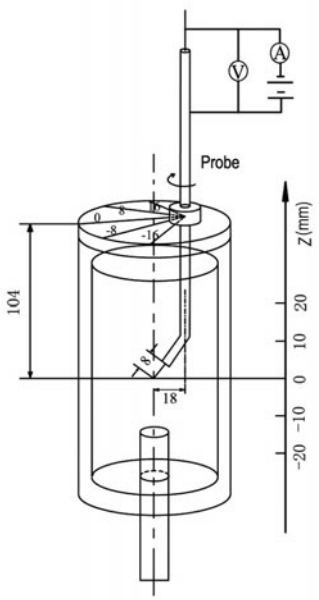

Fig.2 Schematic diagram of internal structure of the reaction chamber and probe

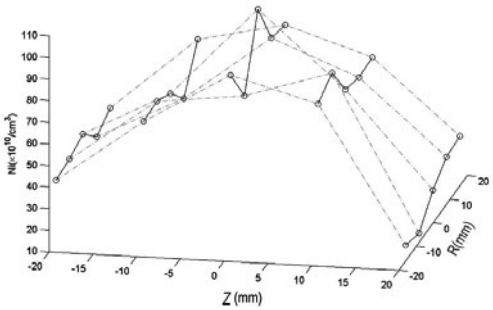

Fig.3 Spatial plasma density distribution

$$N_{\mathrm{i}} = \frac{I_{\mathrm{i}0}}{0.61eS(KT_{\mathrm{e}}/m_{\mathrm{i}})^{1/2}},$$

where $I_{\mathrm{i}0}$ is the saturation ion current collected by the probe with a surface area S.

3 Experimental results and discussion

3.1 Spatial plasma density distribution in the reaction chamber

In the reaction chamber, when the gas system 1 into the reaction chamber is CH_4 with a flow rate of 6 mL/min and the gas system 2 into the reaction chamber is H_2 with a flow rate of 200 mL/min and a microwave power $P_{\mathrm{w}} = 440$ W, $p = 1.20$ kPa, we obtained the spatial plasma density distribution, by using the Langmuir probe, at the axial positions $Z = -20$ mm, -10 mm, 0 mm, 10 mm, 20 mm and at the radial positions $R = -16$ mm, -8 mm, 0 mm, 8 mm, 16 mm, as shown in Fig. 3.

As shown in Fig. 3 , at $Z = 0$, $R = 0$, the plasma density is the highest, reaching $1.05 \times 10^{12}/\mathrm{cm}^3$. This is because in the energy transfer pattern of the waveguide

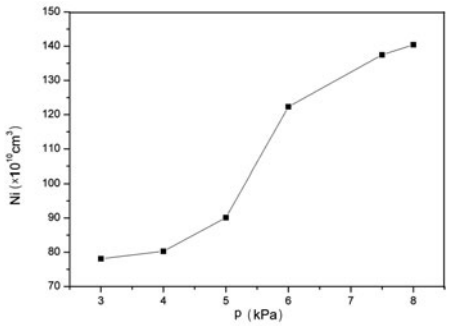

Fig.4 Plasma density under different gas pressures

BJ22, the microwave is coupled to the middle of the quartz tube reaction chamber, generating the highest wave energy at this position and exciting more neutral particles.

At $Z = -20$ mm, -10 mm, 0 mm, 10 mm and 20 mm, the plasma density uniformity is 76.8%, 73.6%, 70.0%, 77.3% and 42.8% respectively, with the best value 77.3% at $Z = 10$ mm. Therefore, this position was chosen for the film deposition. But at $Z = 20$ mm, due to the influence of the air inlet, the uniformity is worst, at 42.8% only, and is not suitable for film deposition.

3.2 Plasma density under different gas pressures

At $Z = -20$ mm, $R = 0$ mm, with the flow rate of CH_4 of 6 mL/min and H_2 of 200 mL/min, and $P_{\mathrm{w}} = 560$ W, we obtained the plasma density under different gas pressures in the reaction chamber. As shown in Fig. 4, the plasma density increases as the gas pressure increases. This is because the neutral particle density increases along with the increase in the gas pressure. In the electric discharge, the ion is generated by the electron-neutrals' collision, and the average collision frequency between electron and neutral particles is $f = N\sigma v$, with N the neutral gas density, σ the collision cross-section between the electron and the neutral particles and v is the electron velocity. Therefore, when N increases, the collision frequency between the electrons and neutral particles increases. With the rise in ionicity, ionization becomes dominant, and consequently the plasma density increases.

The enhancement of the deposition gas pressure is helpful to the formation of diamond-like carbon films. However, as the gas pressure increases, the temperature will increase [7], causing the graphite growth speed to increase greatly.

3.3 Plasma density under different microwave powers

At $Z = -20$ mm, $R = 0$ mm, with the flow rates of CH_4 of 6 mL/min and H_2 of 200 mL/min, and the pressure $p = 1.16$ kPa, we obtained the plasma density under different powers in the reaction chamber. As shown in Fig. 5, the plasma density increases with the increase

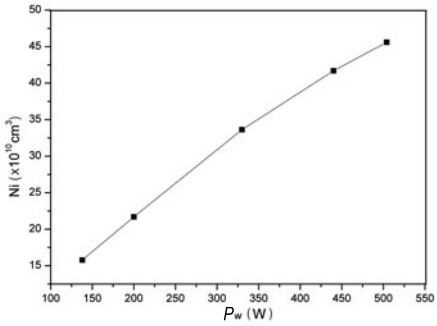

Fig.5 Plasma density under different powers

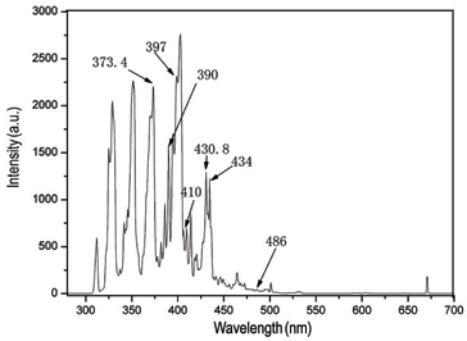

Fig.6 OES from H_2 and CH_4

in power. This is because, as the microwave power increases, the field intensity increases which leads to heat up the electrons and speed up the the electron velocity so as to form energetic electrons. These energetic electrons collide with the neutral particles and cause more neutral particles to be activated and ionized. Hence, when the electrons aquire higher energy, the gas ionization rate increases, and the gas is more activated and ionized.

3.4 OES of H_2 and CH_4 discharge

Fig. 6 shows the OES from H_2 and CH_4 discharge at P_w= 680 W, p = 6.8 kPa, the flow rate of CH_4 of 6 mL/min and the flow rate of H_2 of 200 mL/min. It exhibits H_γ at 434 nm, H_β at 486 nm, H radical at 373.4 nm, 397 nm and 410 nm [8]. The H-H bond breaking-down process of the hydrogen molecule is simple, generating active H through a non-elastic collision with the energetic electron. During the MPCVD process, the existence of hydrogen atoms can help stabilize sp^3, making the carbon atoms maintain the sp^3 hybridization condition in the diamond metastable region. Simultaneously it sculptures the sp^2 carbon bond to restrain the nucleation and the growth of the non-diamond-like graphite and amorphous carbon. Also, hydrogen atoms can make more graphite atoms cross the potential barrier tending to the diamond condition [7].

On the other hand, there are characteristic optical emission spectroscopic lines of CH ($B^2\Sigma \rightarrow X^2\Pi$) at 390 nm and ($A^2\Delta \rightarrow X^2\Pi$) at 430.8 nm [9]. The existence of CH is favorable for the formation of the amorphous carbon layer. As shown in Fig. 6, because of the existence of higher CH concentrations, it will cause more graphite to grow, reducing the sp^3 bonding.

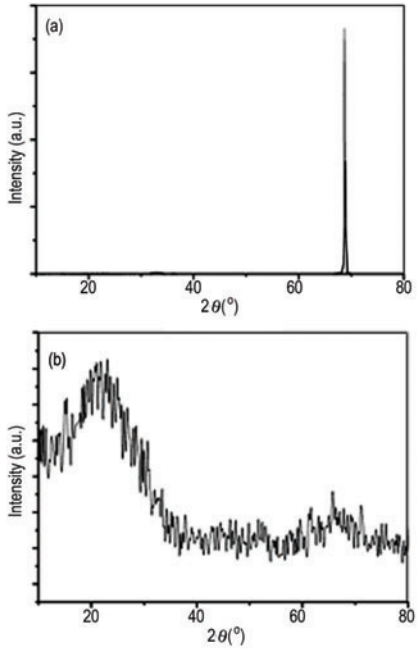

Fig.7 XRD

It is believed that H and CH play important roles in the diamond-like carbon films' deposition processes [10].

3.5 Characterization of diamond-like carbon thin films

With the conditions of: P_w = 680 W, p = 6.8 kPa, the flow rate of CH_4 of 6 mL/min, and the flow rate of H_2 of 200 ml/min, the diamond-like carbon films were deposited at Z = 10 mm for 3 h. As is shown above , the plasma density increases as both the gas pressure and power increase. Therefore, the plasma density is higher at P_w= 680 W, p = 6.8 kPa. Then the film was characterized by XRD, Raman Spectroscopy, AFM and profiler, as shown in Figs. 7, 8, 9 and 10.

Fig. 7(a) is an XRD image of the substrate Si before deposition. There is an obvious diffraction peak which is the characteristic peak of the single crystal Si.

Fig. 7(b) is an XRD image of the prepared diamond-like carbon thin films. There is no obvious diffraction peak but only a wide diffraction package with a diffraction angle of $20^o \sim 40^o$, revealing the amorphous state diffraction characteristics. This indicates that the diamond-like carbon thin film is a kind of amorphous carbon film [11].

Fig. 8 shows the Raman spectrum of the thin films. The scanning scope of the detector is $1300 \sim 1700$ cm^{-1}. As is shown in Fig. 8, there is a wide peak between $1300 \sim 1700$ cm^{-1}. The diamond-like carbon films contain sp^2 and sp^3 bonding [12]. It is a combination of D and G peaks. According to the above OES results, the existence of higher CH radical concentrations causes more graphite to grow, which lowers the sp^3 bonding. Also, as the above analysis

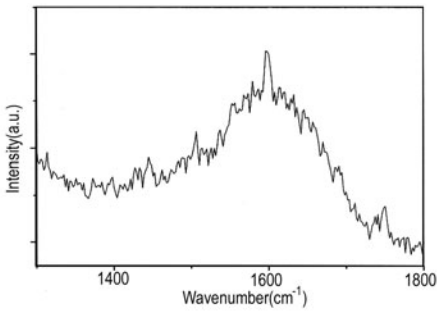

Fig.8 Raman spectrum of diamond-like carbon thin films

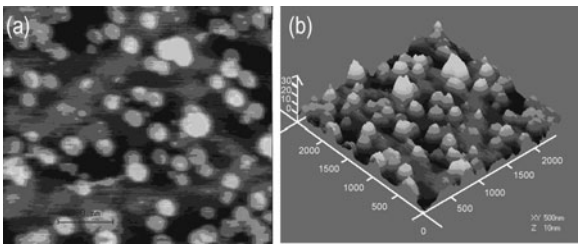

Fig.9 AFM micro images of the diamond-like carbon thin films (a) Plane appearance, (b) Three-dimensional appearance

about the plasma density shows, the film was deposited under a high plasma density at $P_{\mathrm{w}} = 680$ W, $p = 6.8$ kPa. Hence, the growth rate and temperature increase [7] result in an increase in the graphite growth speed. As a result, the D peak is weak compared to the G peak. The existence of D and G peaks corresponds to the results of XRD that the film is amorphous carbon film.

We used the tapping AFM pattern to scan the surface of the films. In this pattern, it is not destructive to the surface. Fig. 9 shows micro-images of the diamond-like carbon thin films, among which (a) is a plane appearance with a scanning scope of 2500 nm × 2500 nm while (b) is a three-dimensional representation of (a). With AFM, we obtain $R_{\mathrm{q}} = 4.5$ nm.

From Fig. 9, we can see that the granule distribution is quite even, with the bigger granules being 200 nm and the smaller being 10 nm. With the profiler, we examined the superficial roughness of the diamond-like carbon thin films, and the surface roughness can be characterized by $R_{\mathrm{q}} = \sqrt{\frac{1}{e}\int_0^i y^2(x)\mathrm{d}x}$. As shown in Fig. 10, we obtained $R_q = 5.5$ nm, which is consistent with the results of AFM of $R_{\mathrm{q}} = 4.5$ nm, indicating that the superficial smoothness of the thin films is good, which corresponds to what we expected as we chose the best uniformity position $Z = 10$ mm to carry out the film deposition.

4 Conclusions

As the uniformity of plasma density plays an important role in the film deposition, it is necessary to study the uniformity. In this work, by diagnosing the spatial plasma density distribution, we found that the uniformity is best at a location of $Z = 10$ mm. As a result, we selected this position to deposit films. Also, by analysing the plasma density under different gas pressures and applied powers, we determined the relationship between the gas pressure and power and deposited film's characters. OES shows the presence of H radical and CH radical, both of which are associated with the deposition of the DLC films. DLC films were achieved and characterized by AFM, X-ray diffraction instrument, Raman spectroscopy and profiler. The results of XRD indicate that the diamond-like carbon thin filmis a kind of amorphous carbon film, corresponding to the results of the Raman spectrum. With the profiler, we obtained $R_{\mathrm{q}} = 5.5$ nm, which is consistent with the results of AFM of $R_{\mathrm{q}} = 4.5$ nm, indicating that the superficial smoothness of the thin films is good.

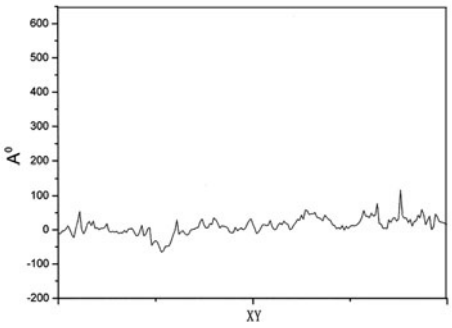

Fig.10 Superficial roughness of the diamond-like carbon thin films

References

1 Musil J. 1996, Vacuum, 47: 145
2 Sanchez N A, Rincon C, Zambrano G, et al. 2000, Thin Solid Films, 373: 247
3 Cicala G, Bruno P, Losacco A M, et al. 2004, Surface and Coatings Technology, 180∼181: 222
4 Chen J F, Ren Z X. 1999, Vacuum, 52: 411
5 Liu P Y, Chen J F, Sun W D. 2004, Vacuum, 76: 7
6 Chen J F, Zhao W F, Wu X Q, et al. 2004, Plasma Science and Technology, 6: 2233
7 Zhou J, Fu W B, Yuan R Z. 2002, Diamond films deposited by Microwave plasma CVD. (Beijing: Building Materials Industry Press), p.33-35, 119, 126 (in Chinese)
8 Ke Y K, Dong H R. 2001, Handbook of Analytical Chemistry (Spectral Analysis). (Beijing: Chemical Industry Press) (in Chinese)
9 Andjuar J L, Pascual E, Viera G, et al. 1983, Thin Solid Films, 317: 120
10 Liao Y, Li C H, Ye Z Y, et al. 2000, Diamond and Related Materials, 9: 1716
11 Cheng Y H, Wu Y P, Chen J G, et al. 1997, Journal of Chinese Ceramic Society, 8: 452 (in Chinese)
12 Yoon S F, Tan K H, Rusli, et al. 2000, Diamond and Related Materials, 9: 2024

(Manuscript received 22 May 2006)
E-mail address of corresponding author
CHEN Junfang: chenjf@scnu.edu.cn